Accepted Manuscript

Synthesis, biological evaluation and molecular docking studies of pyrazole derivatives coupling with a thiourea moiety as novel CDKs inhibitors

Jian Sun, Xian-Hai Lv, Han-Yue Qiu, Yan-Ting Wang, Qian-Ru Du, Dong-Dong Li, Yong-Hua Yang, Hai-Liang Zhu

PII: S0223-5234(13)00441-8

DOI: 10.1016/j.ejmech.2013.07.003

Reference: EJMECH 6290

To appear in: *European Journal of Medicinal Chemistry*

Received Date: 21 April 2013

Revised Date: 7 July 2013

Accepted Date: 8 July 2013

Please cite this article as: J. Sun, X.-H. Lv, H.-Y. Qiu, Y.-T. Wang, Q.-R. Du, D.-D. Li, Y.-H. Yang, H.-L. Zhu, Synthesis, biological evaluation and molecular docking studies of pyrazole derivatives coupling with a thiourea moiety as novel CDKs inhibitors, *European Journal of Medicinal Chemistry* (2013), doi: 10.1016/j.ejmech.2013.07.003.

Synthesis, biological evaluation and molecular docking studies of pyrazole derivatives coupling with a thiourea moiety as novel CDKs inhibitors

Jian Sun [a]†, *Xian-Hai Lv* [b]†, *Han-Yue Qiu* [a], *Yan-Ting Wang* [a], *Qian-Ru Du* [a], *Dong-Dong Li* [a], *Yong-Hua Yang* [a*], *Hai-Liang Zhu* [a*]

[a] *State Key Laboratory of Pharmaceutical Biotechnology, Nanjing University,Nanjing 210093, People's Republic of China*

[b] *College of Science, Anhui Agricultural University, Hefei 230036, People's Republic of China*

[+] These authors contributed equally to this work.

* Corresponding author. Tel.: +86-25-8359 2572; Fax: 0086+25+8359 2672;

E-mail address: zhuhl@nju.edu.cn

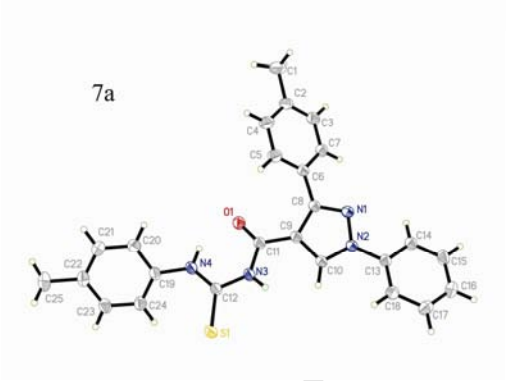

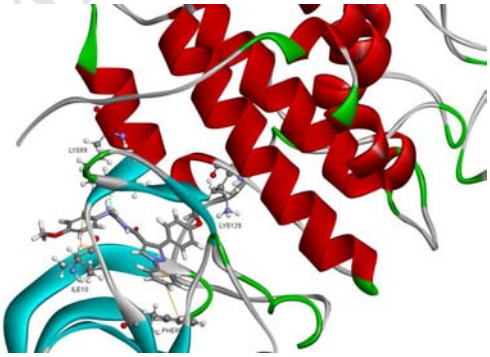

Twenty new pyrazole derivatives have been designed and evaluated for their anticancer and CDKs inhibitory activity. Compound **10b** demonstrated the most potent inhibitory activity.

Synthesis, biological evaluation and molecular docking studies of pyrazole derivatives coupling with a thiourea moiety as novel CDKs inhibitors

Jian Sun [a]†, *Xian-Hai Lv* [b]†, *Han-Yue Qiu* [a], *Yan-Ting Wang* [a], *Qian-Ru Du* [a], *Dong-Dong Li* [a], *Yong-Hua Yang* [a*], *Hai-Liang Zhu* [a*]

[a] *State Key Laboratory of Pharmaceutical Biotechnology, Nanjing University,Nanjing 210093, People's Republic of China*

[b] *College of Science, Anhui Agricultural University, Hefei 230036, People's Republic of China*

[†] These authors contributed equally to this work.

** Corresponding authors. Tel./fax: +86-25-83592672;*

E-mail address: zhuhl@nju.edu.cn

Abstract

It was discovered that a number of cyclin dependent kinase inhibitors containing the pyrazole core structure exhibited high inhibitory potency against broad-range CDKs and corresponding anti-proliferative activities. This information guided us to design and synthesize a series of 1, 3-diphenyl-*N*-(phenylcarbamothioyl)-1*H*-pyrazole-4-carboxamide derivatives (**5a-10d**), and evaluate their biological activities as CDKs inhibitors. Among all the synthesized compounds, compound **10b** inhibited CDK2 with an IC_{50} value of 25 nM, counteracting tumor cell proliferation of three cancer cell lines (H460, MCF-7, A549) in the micromolar range (from 0.75 μM to 4.21 μM), In addition, flow cytometry indicated that compound **10b** could induce cycle G_0/G_1 phase arrest in A549 cells with a dose dependent. Taken together, compound **10b** could be selected for further preclinical evaluation.

Keywords:

Cyclin-dependent kinases;

CDK2;

Cell cycle profile;

Structure-activity relationship;

Molecular docking

Introduction

Along with the living habits and environment changes, cancer has become the major cause of death in both developing and developed countries [1]. Until now one significant way to induce the occurrence of cancers is still by mutation or mis-regulation of cell cycle regulatory genes and proteins to guide an abnormal control of cell proliferation [2]. The cyclin-dependent kinases (CDKs) are a family of serine-threonine protein kinases, which are key regulatory elements in cell cycle progression. Inhibition of CDKs activity has turned out to be the most effective strategy for the discovery of novel anticancer agents specifically targeting the cell cycle proteins [3]. To this end, we attempted to design and synthesize new molecule inhibitors targeting these kinases and related kinase-overexpression cancers.

CDK2, one significant member of CDKs family, have been proved to participate in the majority of cancer cases mainly due to it could play a vital role during the G1/S transition of the cell cycle when combined with cyclin E. Besides, plenty of reports also illustrated that the inhibition of CDK2 could be an important way for the treatment of cancers [4-5]. However, recent evidences indicated that the highly selective inhibitors of individual CDK may not be therapeutically effective because of the functional redundancy within the CDK family [6]. Additionally, several small molecule candidates which have already undergone clinical evaluation are all broad-range CDKs inhibitors which could meanwhile inhibit more than one member of the CDK family [7-9]. Here are some representative compounds illustrated in **Figure 1**, such as PNU-292137 (CDK1, 2, 4 inhibitor), 1*H*-indazole-3-carboxylic acid (4-sulfamoylphenyl)amide (CDK1, 2 inhibitor), AT7519 (CDK1, 2, 4, 5 inhibitor), olomoucine (CDK1, 2, 5 inhibitor), and roscovitine (CDK1, 2, 5, 7 inhibitor) [2].

(Fig 1)

In terms of the mechanism that the development of new anticancer therapeutic agents is one of the fundamental goals in medicinal chemistry field, we tried to design a series of novel broad-range CDKs inhibitors. As shown above, three inhibitors (PNU-292137, 1*H*-indazole-3-carboxylic acid (4-sulfamoylphenyl)amide, AT7519) shared the same pyrazole scaffold that facilitates us preliminarily in considering the pyrazole core as the basic skeleton for designing novel pan-CDKs inhibitors as

antitumor agents. Besides, given the remarkable pharmacological activities (antibacterial, antifungal, tumor necrosis and antiangiogenic) of pyrazole derivatives, [10-13] and those inhibitors coupling with pyrazole ring reported by Brasca *et al.* [6] displayed highly activity against various CDKs and impressive selectivity against a panel of serine-threonine and tyrosine kinases, we envisioned pyrazole ring actually is a promising skeleton when involved in the inhibition of CDKs in cell cycle progression. Thus, we attempted to design a series of pyrazole derivatives as broad-range CDKs inhibitors.

With respect to the linkers between the core and the hydrophobic blocks of designed compounds in the ATP-binding sites of CDKs proteins, we attempted to employ the common thiourea linkers. It is noted that this linker as well as amido linkage could bind tightly to the hinge part of the binding site, forming several various interactions with certain important residues, such as hydrogen bond, or charge interaction. In addition, thiourea derivatives have attracted continuing interest over the years because they displayed a wide range of biological activity including anti-fungal, antibacterial, insecticidal, antitubercular, herbicidal, and plant growth regulator properties [14-16]. Especially recent years, thiourea derivatives with their antitumor activity have become a new hot spot. Such as diarylsulfonylurea derivatives [17-18] have been reported to possess a broad spectrum of anticancer activity in several tumor models and showing good growth inhibition; hydroxyurea [19] has been described as a clinically useful drug for the treatment of a wide range of solid tumors. Besides, our previous research have illustrated that 1-(3-chloro-2-hydroxybenzyl)-1-(4-hydroxybenzyl)-3-phenylthiourea possessed remarkable anti-proliferative activity [20].

But to our knowledge, few reports have been dedicated to design and synthesize an antitumor compound which contains pyrazole and thiourea simultaneously. The pyrazole ring along with the thiourea ring, the two combined substructures, might exhibit synergistic anticancer effect. All of these encouraged us to integrate these two structures and screen new pyrazole-thiourea derivatives as potential broad-range CDKs inhibitory agents. Herein, we described the synthesis and the structure-activity relationship (SAR) of 1, 3-diphenyl-*N*-(phenylcarbamothioyl)-1H-pyrazole-4-carboxamide derivatives. Biological evaluation indicated that some of the targeted compounds could be potential inhibitors of broad-range CDKs. Docking simulations

were performed using the X-ray crystallographic structure of the CDK2 in complex with an inhibitor to explore the binding modes of these compounds at the active site.

2. Results and discussion

2.1. Chemistry

The synthetic route of the cyanic 1, 3-diphenyl-1*H*-pyrazole-4-carboxylic thioanhydride derivatives (**6-10**) was outlined in **Scheme 1**. [3, 21] Compounds **6-10** were prepared by the simple condensation and cyclization of phenylhydrazine and various substituted acetophenones.

The synthetic route of 1, 3-diphenyl-*N*-(phenylcarbamothioyl)-1*H*-pyrazole-4-carboxamide derivatives (**6a-10d**) was shown in **Scheme 2**. [21] As reports, the synthesis of compounds (**6a-10d**) began with the interaction of substituted cyanic 1, 3-diphenyl-1*H*-pyrazole-4-carboxylic thioanhydride and substituted anilines with the help of K_2CO_3 in anhydrous methylene dichloride.

(Scheme 1)

(Scheme 2)

These compounds were all reported for the first time. All of the synthesized compounds **6a-10d** (**Table 1**) gave satisfactory elementary analytical and spectroscopic data. ^{1}H NMR, ^{13}C NMR and ESI-MS spectra were consistent with the assigned structures. Additionally, the structure of compound **7a** was further confirmed by X-ray diffraction. Its crystal data were presented in **Table 2** and **Figure 2** gave a perspective view of this compound together with the atomic labeling system.

(Table 1)

(Table 2)

(Fig. 2)

2.2. Bioassay

To test the anticancer activities of the synthesized compounds, we evaluated anti-proliferative activities of compounds **6a-10d** against A549 (carcinomic human alveolar basal epithelial cell), MCF-7 (breast cancer cell line) and H460 (lung carcinoma cell line). The results were summarized in **Table 3**. With few exception, the active analogs showed a remarkable potential antitumor activity, suggesting that 1, 3-diphenyl-*N*-(phenylcarbamothioyl)-1*H*-pyrazole-4-carboxamide derivatives could significantly enhance anticancer potency. For the given compounds, it was observed that compound **10b** showed the most potent biological activity (IC_{50} = 2.57 ± 0.12 μM for H460 and IC_{50} = 0.75 ± 0.03 μM for A549).

According to the data presented in **Table 3**, we could arrive at the conclusion that the activity of the tested compounds may be correlated to the variation and modifications of structure. For instance, different substitutes on the A-ring determine the primary order of potency. Among the compounds, the compounds with OMe and Me group as electron-donating substituents on ring A were of better antitumor activity comparing to those with electron-withdrawing, the potency of para-substituents on the A-ring was ordered as: OMe > Me > H > F> Cl. In addition, change of substituents on the B-ring under constant A-ring substituents could also affect the activities of these compounds. A comparison of the para-substituents on the B-ring demonstrated that OMe group could dramatically improve anti-proliferative activity, with the presumption that OMe group at the para-position of ring B might bind potently into targeting protein. An overview of the compounds, compounds **10b** meanwhile have para-OMe group on the A-ring and para-OMe on the B-ring. Therefore, it displayed the most potent anticancer activity.

On the basis of previous research, it was revealed that the class of *N*-((1, 3-diphenyl-1*H*-pyrazol-4-yl)methyl)aniline inhibitors possessed exclusively CDK2 inhibitory activity. [3] To examine whether the synthesized compounds could also inhibit CDK2, we screened compounds **6a-10d** against the CDK2. An analysis of the potency data we obtained by screening compounds **6a-10d** against the CDK2 (**Table 3**), the analysis results manifested that compounds **7b**, **8b** and **10b** showed strong inhibitory effect (IC_{50} = 0.047 μM, 0.037 μM and 0.025 μM, respectively) and the IC_{50} values of enzyme assay shared a similar tendency with that of anti-proliferative assay. These results indicated the anti-proliferative effect might be produced partly by interaction between CDK2 protein and the compounds. An analysis between the anti-proliferative activity against A549 cell line and the CDK2 inhibitory activity of 8

compounds (**6b, 7b, 8b, 9b, 10a, 10b, 10c,** and **10d**) verified that there indeed was a moderate correlation between CDK2 inhibition and inhibition of cancer cellular proliferation, as evidenced in **Figure 3**, with a R square value 0.84.

(Table 3)

(Fig. 3)

To further investigate kinase selectivity of these compounds for CDKs, compounds **6b, 7b, 8b, 9b**, and **10b** were evaluated as potential inhibitors of other seven protein kinases relevant to cancers: CDK1, CDK4, CDK5, CDK6, CDK7, EGFR, and VEGFR2. Complexes of CDK1 can regulate both the G2 to M phase transition and mitosis; CDK2, CDK4 and CDK6 primarily regulate progression from the G1 (Gap1) phase to the S phase (DNA synthesis) of the cell cycle; CDK5 plays a role in neuronal and secretory cell function; CDK7 is a component of the CDK-activating kinase (CAK), which acts upstream of cell-cycle CDKs; [22] EGFR is the cell-surface receptor for members of the epidermal growth factor family of extracellular protein ligands; [23] VEGFR2 is a receptor tyrosine kinase expressed on the endothelial cells which can mediate endothelial cell proliferation, differentiation, and micro-vascular permeability. [24] As expected, the results in **Table 4** showed that all the selected compounds (**6b, 7b, 8b, 9b,** and **10b**) lowered at least one order of magnitude in the inhibition for EGFR and VEGFR2, when compared to CDKs. Besides, the data of **Table 4** also demonstrated that those five compounds would prefer to CDK2, CDK4, CDK6 (IC_{50} : 25-50 nM) than the other three members CDK1, CDK5 and CDK7 (IC_{50} : 500-2000 nM). Therefore, we tended to conclude that the synthesized molecule inhibitors can blockade the function of CDK2, CDK4, CDK6 and might have involved in the process of G1 to S phase transition of the cell cycle. The detailed results were summarized in **Table 4**.

(Table 4)

To gain better understanding on the preliminary mechanism of the studied compounds with potent inhibitory activity, the cell cycle profile experiment was performed to assay the effect of compound **10b** in **Figure 4**. The cell cycle profile of

the treated cells showed obvious effect at micromolar range: a subsequent increase of the G_0/G_1 population compared to the control cells. The presence of cells with G_0/G_1 DNA content (from 57.07% in control cells to 64.00% in cells treated with compound **10b** at 2 μM). This result indicated that compound **10b** could induce cycle G_0/G_1 phase arrest and affect G1 to S phase transition.

(Fig. 4)

2.3. Molecular docking

Paul group [25] given a detail analysis of the ATP binding site of CDK2 (PDB code: 2VTO) and identified a number of key regions including a hydrophobic pocket (defined by Ile10, Phe82, Asp86, and Leu134); the relatively small region between the gatekeeper residue (Phe80) and the DFG motif (Asp145) and the solvent accessible region toward Lys89.

A docking study was performed to fit compound **10b** and reference compound **(LZ8)** [25] into the active center of 2VTO. The obtained results were presented in Figures 5. **Figures 5A** and **5B** showed the binding mode of compound **10b** interacting with 2VTO protein and the docking results revealed that three amino acids Phe80, Asp86, Lys89 located in the binding pocket of protein played a vital roles in the combination with compound **10b**, which were stabilized by one Pi-Pi bond, two hydrogen bonds. One Pi-Pi bond, of which their lengths were 4.5 Å, was formed by the C ring and Phe80; One hydrogen bond was provided by the nitryl group beside A ring and Asp86 while another hydrogen bond was involved in thiourea linkers and Lys89 which verified that thiourea linkers could bind tightly to active center and employing thiourea structure was reasonable. **Figure 5C** and **5D** displayed 2D and 3D interactional maps between compound **LZ8** and CDK2 protein crystal structure. Insight into this picture, we can see that only one hydrogen bond which was consisted by nitryl and Leu83 involved in the binding between the compound and the active site. Therefore, we anticipated compound **10b** could well embed in the active pocket and have much better physicochemical properties than reference compound **LZ8**. In addition, the enzyme surface model was showed in **Figure 6**, which revealed that the molecule **10b** occupies the ATP-binding pocket and binds to an active conformation of CDK2.

(Fig. 5)

(Fig. 6)

3. Conclusion

In this study, a series of 1, 3-diphenyl-*N*-(phenylcarbamothioyl)-1*H*-pyrazole-4-carboxamide derivatives have been synthesized and evaluated for their antitumor activities. These compounds exhibited potent anti-proliferative activities against A549 and CDK2, 4, 6 inhibitory activities. Among all of the synthesized compounds, compound **10b** demonstrated the most potent inhibitory activity (IC_{50} of 25 nM, 35 nM, 29 nM for CDK2, 4, 6). Anti-proliferative assay results also showed that compound **10b** (IC_{50} = 0.75 μM for A549) had the potential to be developed as a anti-proliferative agent against A549. Docking simulation was performed to position compound **10b** into the human CDK2 active site to determine the probable binding model. Analysis of the compound **10b** binding conformation in active site showed that the compound **10b** was stabilized by one Pi-Pi bond with PHE80 and two hydrogen bonds, respectively, with ASP86 and LYS89. Cell cycle profile experiment also showed the compound **10b** was a potential antitumor agent. The information of this work might be helpful for the design and synthesis of a leading compound **10b** towards the development of new therapeutic agent to fight against cancer.

4. Experimental Section

4.1. Materials and Methods.

All of the synthesized compounds were chemically characterized by thin layer chromatography (TLC), proton nuclear magnetic resonance (^{1}H NMR) and elemental microanalyses (CHN). ^{1}H NMR spectra were measured on a Bruker AV-300 or AV-500 spectrometer at 25 □ and referenced to Me_4Si. Chemical shifts were reported in ppm (δ) using the residual solvent line as internal standard. Splitting patterns were designed as s, singlet; d, doublet; t, triplet; m, multiplet. ESI-MS spectra were recorded on a Mariner System 5304 Mass spectrometer. Elemental analyses were performed on a CHN-O-Rapid instrument and were within ± 0.4 % of the theoretical values. Melting points were determined on a XT4 MP apparatus (Taike Corp., Beijing,

China) and were as read. Analytic thin-layer chromatography (TLC) was performed on the glass-backed silica gel sheets (silica gel 60 Å GF254). All compounds were detected using UV light (254 nm or 365 nm).

4.2. General method for the preparation of target compounds 6-10

The starting material substituted 1, 3-diphenyl-1*H*-pyrazole-4-carboxylic thioanhydride derivatives **(6-10)** was synthesized as following: para-substituted acetophenone **(1-5)** (20 mmol) interact with phenylhydrazine hydrochloride (25 mmol) couple with sodium acetate (40 mmol) in anhydrous ethanol to form 1-phenyl-2-(1-phenylethyli-dene) hydrazine, which was then dissolved in a cold mixed solution of DMF (20 mL) and $POCl_3$ (16 mL), stirred at 50-60 °C for 5 h. The resulting mixture was poured into ice-cold water, a saturated solution of sodium hydroxide was added to neutralize the mixture, then the obtained solid precipitate were oxidized to the corresponding carboxylic acids by treatment with potassium permanganate (10 mmol), stirred at 70-80 °C for 3 h. while the transformation of acids into the appropriate acid chlorides was accomplished with thionyl chloride in refluxing toluene for 3 h. A solution of substituted acid chlorides (4 mmol) in anhydrous acetone (10 ml) and 3% TBAB in acetone was added drop wise to a suspension of ammonium thiocyanate in acetone (10 ml) and the reaction mixture was refluxed for 1 h to give the desired compounds **6-10.**

4.3. General procedure for 1,3-diphenyl-*N*-(phenylcarbamothioyl)-1*H*-pyrazole-4-carboxamide derivatives (6a-10d)

Compounds **6a-10d** were synthesized from a stirring mixture of the starting material substituted 1, 3-diphenyl-1*H*-pyrazole-4-carboxylic thioanhydride derivatives **(6-10)** (2 mmol) and substituted anilines (2 mmol) with the help of K_2CO_3 in anhydrous methylene dichloride (15ml) at the room temperate for 1 h. The reaction mixture was poured into five times its volume of cold water when the thiourea precipitated as a solid. The solid product was washed with water and purified by recrystallization from an ethanol-dichloromethane mixture (1:2).

4.3.1

1,3-Diphenyl-*N*-(p-tolylcarbamothioyl)-1*H*-pyrazole-4-carboxamide (6a)

Mp: 175-177□; ^{1}H NMR (300 MHz, $CDCl_3$, δ ppm): 2.28 (s, 3H), 7.12 (d, J = 8.40 Hz, 2H), 7.34 (t, J = 7.22 Hz, 1H), 7.43-7.55 (m, 7H), 7.66 (dd, J_1 = 2.10 Hz, J_2 = 1.20 Hz, 2H), 7.72 (d, J = 8.10 Hz, 2H), 8.55 (s, 1H), 8.67 (s, 1H), 12.28 (s, 1H). ^{13}C NMR (100 MHz, DMSO-d_6, δ ppm): 179.55, 163.92, 153.63, 139.19, 136.11, 135.84, 133.29, 132.30, 130.29, 129.55, 129.34, 129.16, 128.59, 128.00, 124.81, 119.39, 114.62, 21.09. MS (ESI): 412.14 ($C_{24}H_{20}N_4OS$, $[M+H]^+$). Anal. Calcd for $C_{24}H_{19}N_4OS$: C, 69.88; H, 4.89; N, 13.58 Found: C, 69.80; H, 4.85; N, 13.68.

4.3.2

***N*-((4-methoxyphenyl)carbamothioyl)-1,3-diphenyl-1*H*-pyrazole-4-carboxamide (6b)**

Mp: 177-179□; ^{1}H NMR (300 MHz, $CDCl_3$, δ ppm): 3.30 (s, 3H), 7.27-7.35 (m, 6H), 7.45 (t, J = 8.22 Hz, 2H), 7.51-7.58 (m, 4H), 7.70 (d, J = 8.07 Hz, 2H), 8.53 (s, 1H), 8.71 (s, 1H), 12.43 (s, 1H). ^{13}C NMR (100 MHz, DMSO-d_6, δ ppm): 179.56, 163.95, 158.86, 153.63, 139.82, 132.81, 132.31, 130.54, 130.30, 129.75, 129.37, 129.21, 128.57, 127.74, 124.87, 120.34, 114.62, 55.34. MS (ESI): 428.13 ($C_{24}H_{20}N_4O_2S$, $[M+H]^+$). Anal. Calcd for $C_{24}H_{19}N_4O_2S$: C, 67.27; H, 4.70; N, 13.07 Found: C, 67.13; H, 4.53; N, 13.37.

4.3.3

***N*-((4-fluorophenyl)carbamothioyl)-1,3-diphenyl-1*H*-pyrazole-4-carboxamide (6c)**

Mp: 137-139□; ^{1}H NMR (300 MHz, $CDCl_3$, δ ppm): 6.96 (t, J = 8.43 Hz, 2H), 7.07 (t, J = 8.43 Hz, 2H), 7.34-7.79 (m, 10H), 8.62 (s, 1H), 8.78 (s, 1H), 12.39 (s, 1H). ^{13}C NMR (100 MHz, DMSO-d_6, δ ppm): 179.55, 163.96, 162.87, 153.62, 139.84, 134.06, 132.83, 131.23, 130.79, 129.36, 129.23, 127.75, 127.59, 124.86, 120.26, 115.67, 114.61. MS (ESI): 416.11 ($C_{23}H_{17}FN_4OS$, $[M+H]^+$). Anal. Calcd for $C_{23}H_{16}FN_4OS$: C, 66.33; H, 4.11; N, 13.45 Found: C, 66.31; H, 4.01; N, 13.65.

4.3.4

***N*-((4-chlorophenyl)carbamothioyl)-1,3-diphenyl-1*H*-pyrazole-4-carboxamide (6d)**

Mp: 184-186□; ^{1}H NMR (300 MHz, $CDCl_3$, δ ppm): 7.33 (t, J = 8.22 Hz, 2H), 7.43 (t, J = 7.50 Hz, 2H), 7.50-7.80 (m, 10H), 8.63 (s, 1H), 8.74 (s, 1H), 12.49 (s, 1H). ^{13}C NMR (100 MHz, DMSO-d_6, δ ppm): 179.55, 163.91, 153.63, 139.85, 136.62, 133.65,

132.84, 131.26, 130.78, 129.35, 129.22, 129.07, 127.74, 124.85, 120.25, 115.58, 114.62. MS (ESI): 432.08 ($C_{23}H_{17}ClN_4OS$, $[M+H]^+$). Anal. Calcd for $C_{23}H_{16}ClN_4OS$: C, 63.81; H, 3.96; N, 12.94 Found: C, 63.51; H, 3.91; N, 12.99.

4.3.5

1-Phenyl-3-(p-tolyl)-*N*-(p-tolylcarbamothioyl)-1*H*-pyrazole-4-carboxamide (7a)

Mp: 182-184□; ^{1}H NMR (300 MHz, $CDCl_3$, δ ppm): 2.35 (s, 3H), 2.45 (s, 3H), 7.19 (d, J = 8.25 Hz, 2H), 7.37-7.53 (m, 7H), 7.61 (d, J = 8.04 Hz, 2H), 7.78 (d, J = 8.22 Hz, 2H), 8.61 (s, 1H), 8.80 (s, 1H), 12.37 (s, 1H). ^{13}C NMR (100 MHz, DMSO-d_6, δ ppm): 179.55, 164.03, 153.62, 139.22, 138.59, 136.10, 135.84, 133.24, 130.27, 129.56, 129.43, 129.21, 129.16, 127.93, 124.78, 119.36, 114.51, 21.39, 21.09. MS (ESI): 426.15 ($C_{25}H_{22}N_4OS$, $[M+H]^+$). Anal. Calcd for $C_{25}H_{21}N_4OS$: C, 70.40; H, 5.20; N, 13.14 Found: C, 70.06; H, 5.34; N, 13.18.

4.3.6

***N*-((4-methoxyphenyl)carbamothioyl)-1-phenyl-3-(p-tolyl)-1*H*-pyrazole-4-carboxamide (7b)**

Mp: 181-183 □; ^{1}H NMR (300 MHz, $CDCl_3$, δ ppm): 2.45 (s, 3H), 3.81 (s, 3H), 6.91 (q, J = 6.96 Hz, 2H), 7.37-7.59 (m, 7H), 7.61 (d, J = 8.04 Hz, 2H), 7.80 (d, J = 8.07 Hz, 2H), 8.61 (s, 1H), 8.80 (s, 1H), 12.29 (s, 1H). ^{13}C NMR (100 MHz, DMSO-d_6, δ ppm): 179.55, 164.03, 159.34, 153.62, 139.76, 136.21, 135.83, 133.24, 130.84, 129.65, 129.57, 128.46, 127.59, 124.77, 121.21, 119.93, 114.52, 55.75, 21.08. MS (ESI): 442.15 ($C_{25}H_{22}N_4O_2S$, $[M+H]^+$). Anal. Calcd for $C_{25}H_{21}N_4O_2S$: C, 67.85; H, 5.01; N, 12.66 Found: C, 67.63; H, 5.08; N, 12.56.

4.3.7

***N*-((4-fluorophenyl)carbamothioyl)-1-phenyl-3-(p-tolyl)-1*H*-pyrazole-4-carboxamide (7c)**

Mp: 172-174□; ^{1}H NMR (300 MHz, $CDCl_3$, δ ppm): 2.47 (s, 3H), 7.09 (t, J = 8.58 Hz, 2H), 7.39-7.65 (m, 9H), 7.80 (d, J = 8.07 Hz, 2H), 8.62 (s, 1H), 8.80 (s, 1H), 12.42 (s, 1H). ^{13}C NMR (100 MHz, DMSO-d_6, δ ppm): 179.54, 164.05, 163.23, 153.63, 139.78, 136.23, 135.83, 133.25, 130.21, 129.66, 129.52, 128.45, 124.78, 121.23, 119.94, 115.74, 114.51, 21.13. MS (ESI): 430.13 ($C_{24}H_{19}FN_4OS$, $[M+H]^+$). Anal. Calcd for $C_{24}H_{18}FN_4OS$: C, 66.96; H, 4.45; N, 13.01 Found: C, 66.61; H, 4.60; N, 13.06.

4.3.8

***N*-((4-chlorophenyl)carbamothioyl)-1-phenyl-3-(p-tolyl)-1*H*-pyrazole-4-carboxamide (7d)**

Mp: 181-183□; ^{1}H NMR (300 MHz, $CDCl_3$, δ ppm): 2.39 (s, 3H), 6.91 (d, J = 8.94 Hz, 2H), 7.38-7.80 (m, 11H), 8.62 (s, 1H), 8.77 (s, 1H), 12.28 (s, 1H). ^{13}C NMR (100 MHz, DMSO-d_6, δ ppm): 179.86, 164.01, 163.23, 153.64, 139.76, 136.54, 135.84, 133.65, 130.23, 129.65, 129.18, 128.46, 124.77, 121.24, 119.93, 115.75, 114.53, 21.09. MS (ESI): 446.10 ($C_{24}H_{19}ClN_4OS$, $[M+H]^+$). Anal. Calcd for $C_{24}H_{18}ClN_4OS$: C, 64.49; H, 4.28; N, 12.54 Found: C, 64.35; H, 4.29; N, 12.44.

4.3.9

3-(4-Chlorophenyl)-1-phenyl-*N*-(p-tolylcarbamothioyl)-1*H*-pyrazole-4-carboxamide (8a)

Mp: 182-184□; ^{1}H NMR (300 MHz, $CDCl_3$, δ ppm): 2.35 (s, 3H), 7.20 (d, J = 8.22 Hz, 2H), 7.39-7.72 (m, 9H), 7.76 (t, J = 8.04 Hz, 2H), 8.59 (s, 1H), 8.78 (s, 1H), 12.30 (s, 1H). ^{13}C NMR (100 MHz, DMSO-d_6, δ ppm): 179.78, 164.21, 153.63, 139.77, 137.25, 135.56, 134.43, 133.25, 131.22, 129.68, 129.36, 129.28, 128.99, 126.57, 124.74, 119.91, 114.52, 21.08. MS (ESI): 446.10 ($C_{24}H_{19}ClN_4OS$, $[M+H]^+$). Anal. Calcd for $C_{24}H_{18}ClN_4OS$: C, 64.49; H, 4.28; N, 12.54 Found: C, 64.35; H, 4.29; N, 12.44.

4.3.10

3-(4-Chlorophenyl)-*N*-((4-methoxyphenyl)carbamothioyl)-1-phenyl-1*H*-pyrazole-4-carboxamide (8b)

Mp: 203-204□; ^{1}H NMR (300 MHz, $CDCl_3$, δ ppm): 3.80 (s, 3H), 6.87 (d, J = 8.97 Hz, 2H), 7.27-7.79 (m, 11H), 8.55 (s, 1H), 8.77 (s, 1H), 12.33 (s, 1H). ^{13}C NMR (100 MHz, DMSO-d_6, δ ppm): 179.86, 164.23, 159.32, 153.65, 139.75, 134.45, 133.26, 131.22, 129.69, 129.36, 129.27, 128.97, 127.56, 124.76, 119.94, 115.11, 114.53, 55.76. MS (ESI): 462.09 ($C_{24}H_{19}ClN_4O_2S$, $[M+H]^+$). Anal. Calcd for $C_{24}H_{18}ClN_4O_2S$: C, 62.27; H, 4.14; N, 12.10 Found: C, 62.15; H, 4.20; N, 12.22.

4.3.11

3-(4-Chlorophenyl)-*N*-((4-fluorophenyl)carbamothioyl)-1-phenyl-1*H*-pyrazole-4-carboxamide (8c)

Mp: 169-171□; ^{1}H NMR (300 MHz, $CDCl_3$, δ ppm): 7.10 (t, J = 8.94 Hz, 2H), 7.44-7.80 (m, 11H), 8.60 (s, 1H), 8.76 (s, 1H), 12.35 (s, 1H). ^{13}C NMR (100 MHz, DMSO-d_6, δ ppm): 179.83, 164.28, 163.32, 153.66, 139.74, 134.47, 134.15, 133.25, 131.27, 129.68, 129.37, 128.65, 124.79, 129.28, 119.96, 115.89, 114.54. MS (ESI): 450.07 ($C_{23}H_{16}ClFN_4OS$, $[M+H]^+$). Anal. Calcd for $C_{23}H_{15}ClFN_4OS$: C, 61.26; H, 3.58; N, 12.43 Found: C, 61.11; H, 3.43; N, 12.48.

4.3.12

3-(4-Chlorophenyl)-*N*-((4-chlorophenyl)carbamothioyl)-1-phenyl-1*H*-pyrazole-4-carboxamide (8d)

Mp: 201-203□; ^{1}H NMR (300 MHz, $CDCl_3$, δ ppm): 7.36-7.73 (m, 11H), 7.79 (d, J = 8.04 Hz, 2H), 8.59 (s, 1H), 8.74 (s, 1H), 12.44 (s, 1H). ^{13}C NMR (100 MHz, DMSO-d_6, δ ppm): 179.89, 164.20, 153.62, 139.75, 136.61, 134.48, 133.27, 131.28, 131.25, 129.78, 129.62, 129.39, 129.23, 128.66, 124.79, 119.97, 114.59. MS (ESI): 466.04 ($C_{23}H_{16}Cl_2N_4OS$, $[M+H]^+$). Anal. Calcd for $C_{23}H_{15}Cl_2N_4OS$: C, 59.11; H, 3.45; N, 11.99 Found: C, 59.07; H, 3.41; N, 11.89.

4.3.13

3-(4-Fluorophenyl)-1-phenyl-*N*-(p-tolylcarbamothioyl)-1*H*-pyrazole-4-carboxamide (9a)

Mp: 200-202□; ^{1}H NMR (300 MHz, $CDCl_3$, δ ppm): 2.37 (s, 3H), 7.22 (d, J = 8.22 Hz, 2H), 7.30-7.55 (m, 7H), 7.73-7.80 (m, 4H), 8.60 (s, 1H), 8.71 (s, 1H), 12.32 (s, 1H). ^{13}C NMR (100 MHz, DMSO-d_6, δ ppm): 179.85, 164.23, 162.88, 153.69, 139.75, 137.24, 135.69, 133.27, 131.56, 130.31, 129.65, 128.14, 126.57, 124.77, 119.41, 115.62, 114.22, 21.09. MS (ESI): 430.13 ($C_{24}H_{19}FN_4OS$, $[M+H]^+$). Anal. Calcd for $C_{24}H_{18}FN_4OS$: C, 66.96; H, 4.45; N, 13.01 Found: C, 66.65; H, 4.51; N, 13.14.

4.3.14

3-(4-Fluorophenyl)-*N*-((4-methoxyphenyl)carbamothioyl)-1-phenyl-1*H*-pyrazole-4-carboxamide (9b)

Mp: 196-198□; ^{1}H NMR (300 MHz, $CDCl_3$, δ ppm): 3.83 (s, 3H), 6.93 (d, J = 8.97 Hz, 2H), 7.30-7.80 (m, 11H), 8.61 (s, 1H), 8.79 (s, 1H), 12.26 (s, 1H). ^{13}C NMR (100 MHz, DMSO-d_6, δ ppm): 179.82, 164.23, 162.85, 153.74, 139.68, 136.24, 135.24, 133.28, 130.91, 130.33, 129.66, 128.62, 127.56, 124.75, 119.95, 115.63, 114.66,

55.79. MS (ESI): 446.12 ($C_{24}H_{19}FN_4O_2S$ $[M+H]^+$). Anal. Calcd for $C_{24}H_{18}FN_4O_2S$: C, 64.56; H, 4.29; N, 12.55 Found: C, 64.71; H, 4.34; N, 12.61.

4.3.15

3-(4-Fluorophenyl)-*N*-((4-fluorophenyl)carbamothioyl)-1-phenyl-1*H*-pyrazole-4-carboxamide (9c)

Mp: 185-187□, ^{1}H NMR (300 MHz, $CDCl_3$, δ ppm): 7.10 (t, J = 8.65 Hz, 2H), 7.28-7.81 (m, 11H), 8.61 (s, 1H), 8.74 (s, 1H), 12.36 (s, 1H). ^{13}C NMR (100 MHz, DMSO-d_6, δ ppm): 179.82, 164.22, 163.35, 153.75, 139.74, 136.24, 135.14, 133.27, 131.28, 130.69, 129.67, 128.63, 127.57, 124.63, 119.46, 115.86, 114.29. MS (ESI): 434.10 ($C_{23}H_{16}F_2N_4OS$ $[M+H]^+$). Anal. Calcd for $C_{23}H_{15}F_2N_4OS$: C, 63.58; H, 3.71; N, 12.90 Found: C, 63.80; H, 3.69; N, 12.92.

4.3.16

***N*-((4-chlorophenyl)carbamothioyl)-3-(4-fluorophenyl)-1-phenyl-1*H*-pyrazole-4-carboxamide (9d)**

Mp: 184-185□, ^{1}H NMR (300 MHz, $CDCl_3$, δ ppm): 7.28-7.57 (m, 6H), 7.66 (d, J = 8.79 Hz, 2H), 7.73-7.80 (m, 5H), 8.61 (s, 1H), 8.70 (s, 1H), 12.46 (s, 1H). ^{13}C NMR (100 MHz, DMSO-d_6, δ ppm): 179.87, 169.24, 162.94, 153.76, 139.75, 137.69, 135.27, 133.75, 131.27, 130.69, 129.68, 128.64, 124.65, 119.96, 116.59, 115.96, 114.31. MS (ESI): 450.07 ($C_{23}H_{16}ClFN_4OS$ $[M+H]^+$). Anal. Calcd for $C_{23}H_{15}ClFN_4OS$: C, 61.26; H, 3.58; N, 12.43 7.11 Found: C, 61.41; H, 3.53; N, 12.53.

4.3.17

3-(4-Methoxyphenyl)-1-phenyl-*N*-(p-tolylcarbamothioyl)-1*H*-pyrazole-4-carboxamide (10a)

Mp: 178-180 □, ^{1}H NMR (300 MHz, $CDCl_3$, δ ppm): 2.36 (s, 3H), 3.99 (s, 3H), 7.11 (d, J = 8.61 Hz, 2H), 7.21 (d, J = 8.40 Hz, 2H), 7.38-7.69 (m, 7H), 7.80 (d, J = 7.50 Hz, 2H), 8.61 (s, 1H), 8.84 (s, 1H), 12.39 (s, 1H). ^{13}C NMR (100 MHz, DMSO-d_6, δ ppm): 179.86, 164.26, 160.74, 153.74, 139.75, 137.29, 135.61, 133.29, 130.32, 129.64, 128.59, 126.58, 125.36, 124.76, 119.98, 115.63, 114.86, 55.75, 21.09. MS (ESI): 442.15 ($C_{25}H_{22}N_4O_2S$ $[M+H]^+$). Anal. Calcd for $C_{25}H_{21}N_4O_2S$: C, 67.85; H, 5.01; N, 12.66 Found: C, 67.60; H, 5.16; N, 12.68.

4.3.18

3-(4-Methoxyphenyl)-*N*-((4-methoxyphenyl)carbamothioyl)-1-phenyl-1*H*-pyrazole-4-carboxamide (10b)

Mp: 170-172 □, ^{1}H NMR (300 MHz, $CDCl_3$, δ ppm): 3.75 (s, 3H), 3.91 (s, 3H), 6.87 (q, *J* = 9.00 Hz 2H), 7.09 (t, *J* = 7.68 Hz, 2H), 7.38-7.71 (m, 7H), 7.79 (d, *J* = 8.04 Hz, 2H), 8.62 (s, 1H), 8.90 (s, 1H), 12.31 (s, 1H). ^{13}C NMR (100 MHz, DMSO-d_6, δ ppm): 179.84, 164.23, 160.69, 153.75, 139.68, 135.64, 133.32, 130.91, 130.84, 129.65, 128.96, 127.56, 125.39, 124.77, 119.96, 115.23, 114.96, 55.74, 55.73. MS (ESI): 458.14 ($C_{25}H_{22}N_4O_3S$ $[M+H]^+$). Anal. Calcd for $C_{25}H_{21}N_4O_3S$: C, 65.48; H, 4.84; N, 12.22 Found: C, 65.25; H, 4.87; N, 12.27.

4.3.19

***N*-((4-fluorophenyl)carbamothioyl)-3-(4-methoxyphenyl)-1-phenyl-1*H*-pyrazole-4-carboxamide (10c)**

Mp: 162-163 □; ^{1}H NMR (300 MHz, $CDCl_3$, δ ppm): 3.90 (s, 3H), 7.00 (t, *J* = 8.84 Hz, 2H), 7.11 (d, *J* = 8.92 Hz, 2H), 7.30-7.70 (m, 7H), 7.78 (d, *J* = 7.89 Hz, 2H), 8.61 (s, 1H), 8.83 (s, 1H), 12.41 (s, 1H). ^{13}C NMR (100 MHz, DMSO-d_6, δ ppm): 179.83, 164.26, 160.68, 153.76, 139.67, 134.23, 133.35, 131.24, 130.92, 129.67, 128.97, 127.64, 125.38, 124.77, 119.97, 115.86, 114.97, 55.75. MS (ESI): 446.12 ($C_{24}H_{19}FN_4O_2S$ $[M+H]^+$). Anal. Calcd for $C_{24}H_{18}FN_4O_2S$: C, 64.56; H, 4.29; N, 12.55 Found: C, 64.32; H, 4.33; N, 12.61.

4.3.20

***N*-((4-chlorophenyl)carbamothioyl)-3-(4-methoxyphenyl)-1-phenyl-1*H*-pyrazole-4-carboxamide (10d)**

Mp: 193-194 □; ^{1}H NMR (300 MHz, $CDCl_3$, δ ppm): 3.90 (s, 3H), 7.11 (d, *J* = 6.75 Hz, 2H), 7.35-7.44 (m, 3H), 7.54 (t, *J* = 7.32 Hz, 2H), 7.66 (d, *J* = 8.76 Hz, 4H), 7.81 (d, *J* = 7.50 Hz, 2H), 8.61 (s, 1H), 8.81 (s, 1H), 12.52 (s, 1H). ^{13}C NMR (100 MHz, DMSO-d_6, δ ppm): 179.86, 164.25, 162.09, 153.76, 139.76, 136.68, 133.75, 131.24, 129.68, 129.14, 128.98, 127.75, 125.69, 124.76, 119.99, 114.99, 114.38, 55.74. MS (ESI): 462.09 ($C_{24}H_{19}ClN_4O_2S$ $[M+H]^+$). Anal. Calcd for $C_{24}H_{18}ClN_4O_2S$: C, 62.27; H, 4.14; N, 12.10 Found: C, 62.41; H, 4.03; N, 12.25.

4.4. **Kinase Assays**

The inhibition studies of cell cycle dependent kinase 1, 2, 4, 5, 6, 7 were performed for the synthesized compounds along with olomoucine and roscovitine as reference compounds. CDK2 enzyme was purified from infected sf21 insect cells. For baculoviral overexpression of proteins, human CDK2 c-DNA tagged by hexa-histidine was subcloned on its N-terminal. CDK2 enzyme was purified using Ni^{2+} affinity resin from sf21 insect cell culture. Enzyme assays were done in 20 mL of 50 mM Tris-HCl containing 10 μM ATP, 0.2 μCi of gamma-P^{32} ATP, 10 mM $MgCl_2$, 5 mM DTT and 4 μg of histone H1 was used as a substrate. The reaction was continued for 10 min in the presence of inhibitors and stopped by adding 10 mL of 30% phosphoric acid. The stopped mixtures were spotted onto P81 paper and were washed with 10 mM Tris-HCl (pH 8.0) containing 0.1 M NaCl for five times. The radioactivity of each spot was quantified with BAS imager. The inhibition studies of human EGFR tyrosine kinase activities were done using C-terminal human EGFR tyrosine kinase domain and Erlotinib was used as a reference compound [26].The inhibition studies of human VEGFR tyrosine kinase activities were done using a DNA sequence encoding the human KDR tyrosine kinase domain (Asp807-Val1356) and ZD-4190 was used as a reference compound [27]. The concentration of inhibitor that gives 50% inhibition was designated as IC_{50} value.

4.5. Cell proliferation assay

CCK8 is much more convenient and helpful than MTT for analyzing cell proliferation, because it can be reduced to soluble formazan by dehydrogenase in mitochondria and has little toxicity to cells. Cell proliferation was determined using CCK8 dye (Beyotime Inst Biotech, China) according to manufacture's instructions. Briefly, 1-5 × 10^3 cells per well were seeded in a 96-well plate, grown at 37 □ for 12 h, Subsequently, cells were treated with compounds (**Table 2**) at increasing concentrations in the presence of 10% FBS for 24 or 48h. After 10 μL CCK8 dye was added to each well, cells were incubated at 37 □ for 1-2 h and Plates were read in a Victor-V multilabel counter (Perkin-Elmer) using the default europium detection protocol. Percent inhibition or IC_{50} values of compounds were calculated by comparison with DMSO-treated control wells. The results are shown in **Table 3**.

4.6. Flow cytometry

Approximately 10^5 cells/well were plated in a 24 well plate and allowed to

adhere. After 12 h, the medium was replaced with fresh culture medium containing compounds **10b** at final concentrations of 0.5, 1, 2 μM. Nontreated wells received an equivalent volume of ethanol (<0.1%). After 36 h, Cells in the supernatant and adherent cells were collected using 0.25% Trypsin, 0.02% EDTA. Cells were washed with PBS and were fixed in 70% ethanol, centrifuged for 1 min at 3000 g at 4 □, washed once with PBS, treated with 1 mg/mL ribonuclease (Sigma Chemical Co.) for 15 min at 37 □ and stained with 50 mg/mL propidium iodide (Sigma Chemi-cal Co.) for 30 min at room temperature. Flow cytometry analyses were performed on a Becton Dickinson FaCS-Calibur using the Becton Dickinson Cell Quest program.

4.7. Docking simulations

The three-dimensional X-ray structure of CDK2 crystal structure (PDB code: 2VTO) was chosen as the template for the modeling study of compound **10b** bound to CDK2. The crystal structure was obtained from the RCSB Protein Data Bank (http://www.rcsb.org/pdb/home/home.do). The molecular docking procedure was performed by using CDOCKER protocol within Discovery Studio 3.1. For ligand preparation, the 3D structure of **10b** was generated and minimized using Discovery Studio 3.1. For protein preparation, the hydrogen atoms were added, and the water and impurities were removed. The molecular docking was performed by inserting compound **10b** into the binding pocket of CDK2 based on the binding mode. Types of interactions of the docked protein with ligand-based pharmacophore model were analyzed after the end of molecular docking.

Acknowledgment

The work was financed by Natural Science Foundation of China (No. J1103512); Universities Natural Science research projects of Anhui Province (KJ2013B088) and the opening foundation of the Key Laboratory of Green Pesticide and Agricultural Bioengineering, Ministry of Education, Guizhou University (No.2011GDGP0105).

References

[1] M. Gallorini,; A. Cataldi,; V. di Giacomo. Biodrugs. 26 (2012) 377-391.

[2] J. Cicenas,; M. Valius. J. Cancer. Res. Clin. 137 (2011) 1409-1418.

[3] X. F. Huang,; X. Lu,; Y. Zhang,; G. Q. Song,;Q. L. He, ; Q. S. Li,; X. H. Yang,; Y. Wei,; H. L. Zhu. Bioorgan. Med. Chem. 20 (2012) 4895-4900.

[4] P. W. Hinds. CANCER CELL. 3 (2003) 305-307.

[5] G. Castanedo,; K. Clark,; S. Wang,; V. Tsui,; M. Wong,; J. Nicholas,; D. Wickramasinghe,; J. C. Marsters,; D. Sutherlina. Bioorg. Med. Chem. Lett. 16 (2006) 1716-1720.

[6] M. G. Brasca,; C. Albanese,; R. Alzani,; R. Amici,; N. Avanzi,; D. Ballinari,; J. Bischoff,; D. Borghi,; E. Casale,; V. Croci,; F. Fiorentini,; A. Isacchi,; C. Mercurio,; M. Nesi,; P. Orsini,; W. Pastori,; E. Pesenti,; P. Pevarello,; P. Roussel,; M. Varasi,; D. Volpi,; A. Vulpetti,; M. Ciomei. Bioorgan. Med. Chem. 18 (2010) 1844-1853.

[7] S. Lapenna,; A. Giordano. Nat. Rev. Drug Discovery. 8 (2009) 547-566.

[8] P. G. Wyatt,; A. J. Woodhead,; V. Berdini,; J. A. Boulstridge,; M. G. Carr,; D. M. Cross. J. Med. Chem. 51 (2008) 4986-4999.

[9] A. Dermatakis,; K. C. Luk,; W. DePinto. Bioorg. Med. Chem. 11 (2003) 1873-1881.

[10] R. Aggarwal,; V. Kumar,; P. Tyagi,; S. P. Singh. Bioorg. Med. Chem. 14 (2006) 1785-1791.

[11] V. Kumar,; R. Aggarwal,; P. Tyagi,; S. P. Singh. Eur. J. Med. Chem. 40 (2005) 922-927.

[12] J. L. Kane,; B. H. Hirth,; O. Laing,; B. B. Gourlie,; S. Nahill,; G. Barsomiam. Bioorg.Med. Chem. Lett. 13 (2003) 4463-4466.

[13] X. H. Liu,; B. F. Ruan,; J. Li. Mini-Rev. Med. Chem. 11 (2011) 771-821.

[14] Y. M. Zhang,; T. B. Wei,; X. C. Wang,; S.Y. Yang. Indian J. Chem. 37 (1998) 604-606.

[15] M. Eweis,; S. S. Elkholy,; M. Z. Elsabee. Int. J. Biol. Macromol. 38 (2006) 1-8.

[16] W. Q. Zhou,; B. L. Li,; L. M. Zhu,; J. G. Ding,; Z. Yong,; L. Lu,; X. Yang. J. J. Mol. Struct. 690 (2004) 145-150.

[17] S. K. Singh,; A. L. Ruchebman,; T. K. Li,; A. Liu,; A. F. Liu,; E. Lavoie. J. J. Med. Chem. 46 (2003) 2254-2257.

[18] A. J. Olaharski,; S. T. Mondrala,; D. A. Eastmond. Mutant Res. 582 (2005) 79-86.

[19] F. Fujita,; M. Fujita,; H. Inaba,; T. Sugimoto,; Y. O kuyama,; T. Taguchi. Gan

To Kagaku Ryoho. 18 (1991) 2263-2270.

[20] H. Q. Li,; T. Yan,; Y. Yang,; L. Shi,; C. F. Zhou,; H. L. Zhu. Bioorgan Med Chem. 18 (2010) 305-313.

[21] S. Saeed,; N. Rashid,; P. G. Jones,; M. Ali,; R. Hussain. Eur. J. Med. Chem. 45 (2010) 1323-1331.

[22] J. Cicenas,; M. Valius. J. Cancer. Res. Clin. 137 (2011) 1409-1418.

[23] Y. Kawakita,; M. Seto,; T.Ohashi,; T. Tamura,; T. Yusa,; H. Miki,; H. Iwata,; H. Kamiguchi,; T. Tanaka,; S. Sogabe,; Y. Ohta,; T Ishikawa. Bioorg. Med. Chem. 21 (2013) 2250-2261.

[24] Y.Oguro,; N. Miyamoto,; K. Okada,; T. Takagi,; H. Iwata,; Y. Awazu,; H. Miki,; A. Hori,; K. Kamiyama,; S. Imamura. Bioorg. Med. Chem. 18 (2010) 7260-7273.

[25] P. G.Wyatt,; A. J. Woodhead,; V Berdini,; J. A. Boulstridge,; M. G. Carr,; D. M. Cross,; D. J. Davis,; L. A. Devine,; T. R. Early,; R. E. Feltell,; E. J. Lewis,; R. L. McMenamin,; E. F. Navarro,; M. A. O'Brien,; M. O'Reilly,; M. Reule,; G Saxty,; L. C. Seavers,; D. M. Smith,; M. S. Squires,; G. Trewartha,; M. T. Walker,; A. J. Woolford. J. Med. Chem. 51 (2008) 4986-4999.

[26] H. S. Ban,; Y. Tanaka,; W. Nabeyama,; M. Hatori,; H. Nakamura. Bioorg. Med. Chem. Lett. 18 (2010) 870-879.

[27] A. Wissner,; M. B. Floyd,; B. D. Johnson,; H. Fraser,; C. Ingalls,; T. Nittoli,; R. G. Dushin,; C. Discafani,; R. Nilakantan,; J. Marini,; M. Ravi,; K. Cheung,; X. Tan,; S. Musto,; T. Annable,; M. M. Siegel,; F. Loganzo. J. Med. Chem. 48 (2005) 7560-7581.

[28] D. A. Ibrahim,; N. Ismail. Eur. J. Med. Chem. 46 (2011) 5825-5832.

Figure caption:

Table 1. Structure of compounds **6a–10d**

Table 2. Crystallographic data and structure refinements for compound **7a**

Table 3. Inhibition (IC_{50}) of A549, MCF-7 and H460 cells proliferation and inhibition of CDK2 by compounds **6a-10d**

Table 4. Selected kinase inhibition activities IC_{50} [a](μM)

Figure 1. ATP-competitive inhibitors of CDKs

Figure 2. Crystal structure of compound **7a**

Figure 3. Correlation between the anti-proliferative activity against A549 cell line and the CDK2 inhibitory activity, R^2 = 0.84, which indicated that there was a moderate correlation between CDK2 inhibition and inhibition of cancer cellular proliferation

Figure 4. Effects of **10b** on the cell cycle distribution in A549 cells. A549 cells were treated with various concentrations of **10b**. A) control; B) concentrations of **10b** was 0.5 μM; C) concentrations of **10b** was 1.0 μM; D) concentrations of **10b** was 2.0 μM. A549 cells were treated with alcohol for 36 h as a control group, Values represent the mean ± S.D, n =3. P <0.05 versus control

Figure 5. A) 2D molecular docking model of compound **10b** with 2VTO; B) Model of compound **10b** bound to CDK2; C) The 2D diagram of docking structure of LZ8 with 2VTO; D) Model of compound **LZ8** bound to CDK2

Figure 6. The surface model of compound **10b** with 2VTO

Scheme 1. Synthesis of compound **6-10**. Reagents and conditions: (i) ethanol, 50-60 °C, 3h; (ii) DMF, $POCl_3$, 50-60 °C, 5 h; (iii) $KMnO_4$, 70-80 °C, 3 h; (iv) $SOCl_2$, toluene, 70-80 °C, 3h; (v) NH_4SCN, 3% TBAB, acetone, rt, 1 h

Scheme 2. Synthesis of compounds **6a-10d**. Reagents and conditions: (i) CH_2Cl_2, K_2CO_3, rt,1 h

Table 1. Structures of compounds **6a-10d**

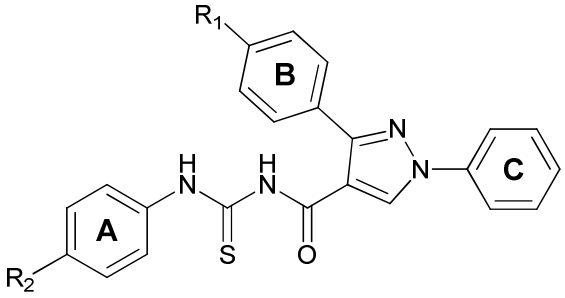

Compounds	R_1	R_2	Compounds	R_1	R_2
6a	H	Me	**8c**	Cl	F
6b	H	OMe	**8d**	Cl	Cl
6c	H	F	**9a**	F	Me
6d	H	Cl	**9b**	F	OMe
7a	Me	Me	**9c**	F	F
7b	Me	OMe	**9d**	F	Cl
7c	Me	F	**10a**	OMe	Me
7d	Me	Cl	**10b**	OMe	OMe
8a	Cl	Me	**10c**	OMe	F
8b	Cl	OMe	**10d**	OMe	Cl

Table 2. Crystallographic data and structure refinements for compound **7a**

Crystal parameters	Compound 7a
Formula	$C_{25}H_{22}N_4OS$
Crystal size (mm)	0.30 x 0.25 x 0.21
Formula weight	426.53
Crystal system	Triclinic
α(°)	89.645(2)
β(°)	80.356(2)
γ(°)	72.588(2)
a(Å)	9.7827(8)
b(Å)	10.2080(8)
c (Å)	11.7098(9)
V (Å3)	1098.81(15)
Z	2

θ limits(°)	2.55≤h≤26.00
hkl limits	-12≤h≤12, -12≤k≤12，-14≤l≤14
F(000)	448
Data/restraints/parameters	4221/0/290
Absorption coefficient	0.172
Reflections collected	10748
Independent reflections	4221 [Rint= 0.0149]
R1/ wR2 [I > 2&Gs(I)]	0.0397/0.1065
R1/wR2 (all data)	0.0444/0.1117
GF	1.022

Table 3. Inhibition (IC_{50}) of A549, MCF-7 and H460 cells proliferation and inhibition of CDK2 by compounds **6a-10d**

Compounds	IC50 (μM)			
	A549 [a]	MCF-7 [a]	H460 [a]	CDK2
6a	2.80±0.16	5.90±0.35	3.96±0.22	0.069±0.0050
6b	2.50±0.14	5.46±0.36	3.54±0.16	0.056±0.0030
6c	3.50±0.23	6.82±0.43	4.21±0.25	0.075±0.0040
6d	3.20±0.21	6.23±0.41	4.02±0.23	0.071±0.0060
7a	2.83±0.19	5.66±0.26	3.76±0.21	0.052±0.0030
7b	2.39±0.16	5.12±0.31	3.24±0.19	0.047±0.0090
7c	3.42±0.33	6.42±0.53	3.98±0.24	0.041±0.0080
7d	3.17±0.27	6.21±0.49	3.65±0.33	0.063±0.0060
8a	2.69±0.18	5.98±0.41	3.12±0.27	0.042±0.0030
8b	2.27±0.22	5.24±0.46	3.01±0.21	0.041±0.0040
8c	3.98±0.43	5.99±0.43	3.64±0.29	0.059±0.0060
8d	3.15±0.29	5.36±0.39	3.26±0.22	0.058±0.0070
9a	2.08±0.17	5.44±0.45	2.98±0.20	0.043±0.0030
9b	1.98±0.14	4.89±0.47	2.86±0.19	0.036±0.0030
9c	3.54±0.26	5.61±0.58	3.24±0.25	0.049±0.0090

9d	2.99±0.18	5.47±0.52	3.09±0.24	0.044±0.0030
10a	1.25±0.11	4.63±0.43	2.88±0.24	0.029±0.0030
10b	0.75±0.03	4.21±0.41	2.57±0.12	0.025±0.0020
10c	1.43±0.09	4.99±0.39	3.05±0.26	0.032±0.0020
10d	1.31±0.14	4.76±0.35	3.01±0.25	0.030±0.0050
Olomoucine	130.00±1.99	142.00±2.12	132.00±2.03	7.00±0.27
Roscovotine	-	-	-	0.50±0.021

[a] Cancer cells kindly supplied by KeyGen Biotech; A549 (carcinomic human alveolar basal epithelial cell), MCF-7 (breast cancer cell line) and H460 (lung carcinoma cell line).

[b] Olomoucine, Roscovotine were prepared according to the literatures [3, 28].

Table 4. Inhibition of selected kinases IC_{50} [a](nM)

Compounds	CDK1	CDK4	CDK5	CDK6	CDK7	EGFR	VEGFR2
6b	610	42	1502	50	1876	>5000	>5000
7b	584	40	1420	43	1788	>5000	>5000
8b	571	40	1356	42	1645	>5000	>5000
9b	569	39	1178	33	1642	>5000	>5000
10b	522	35	1093	29	1423	>5000	>5000

[a] Values are the averages from at least four independent dose response curves;

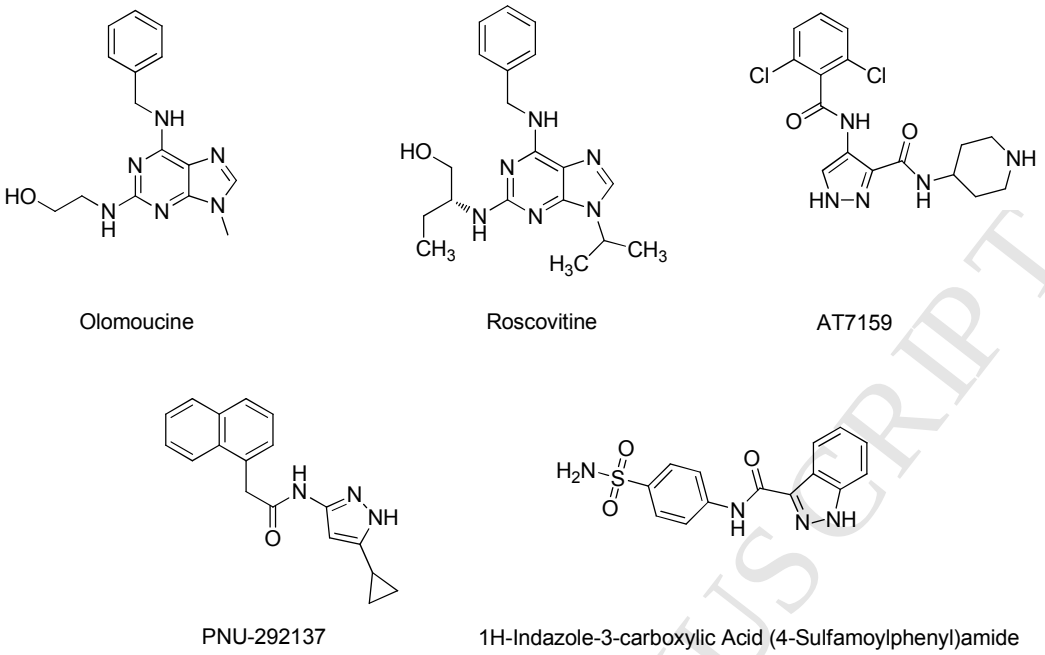

Figure 1. ATP-competitive inhibitors of CDKs

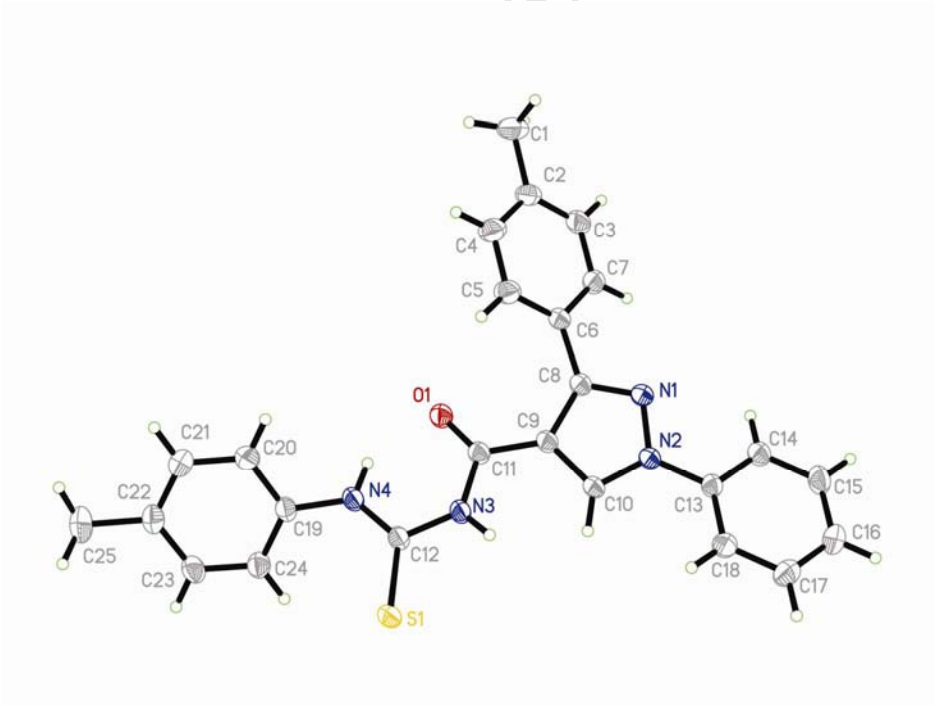

Figure 2. Crystal structure of compound **7a**

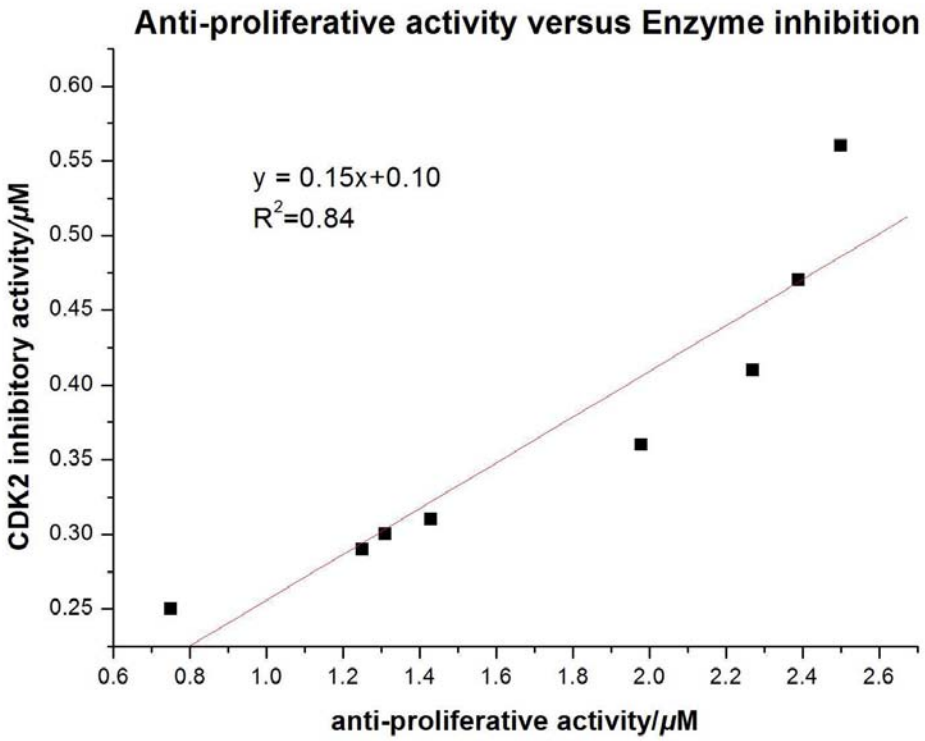

Figure 3. Correlation between the anti-proliferative activity against A549 cell line and the CDK2 inhibitory activity, R^2 = 0.84, which indicated that there was a moderate correlation between CDK2 inhibition and inhibition of cancer cellular proliferation.

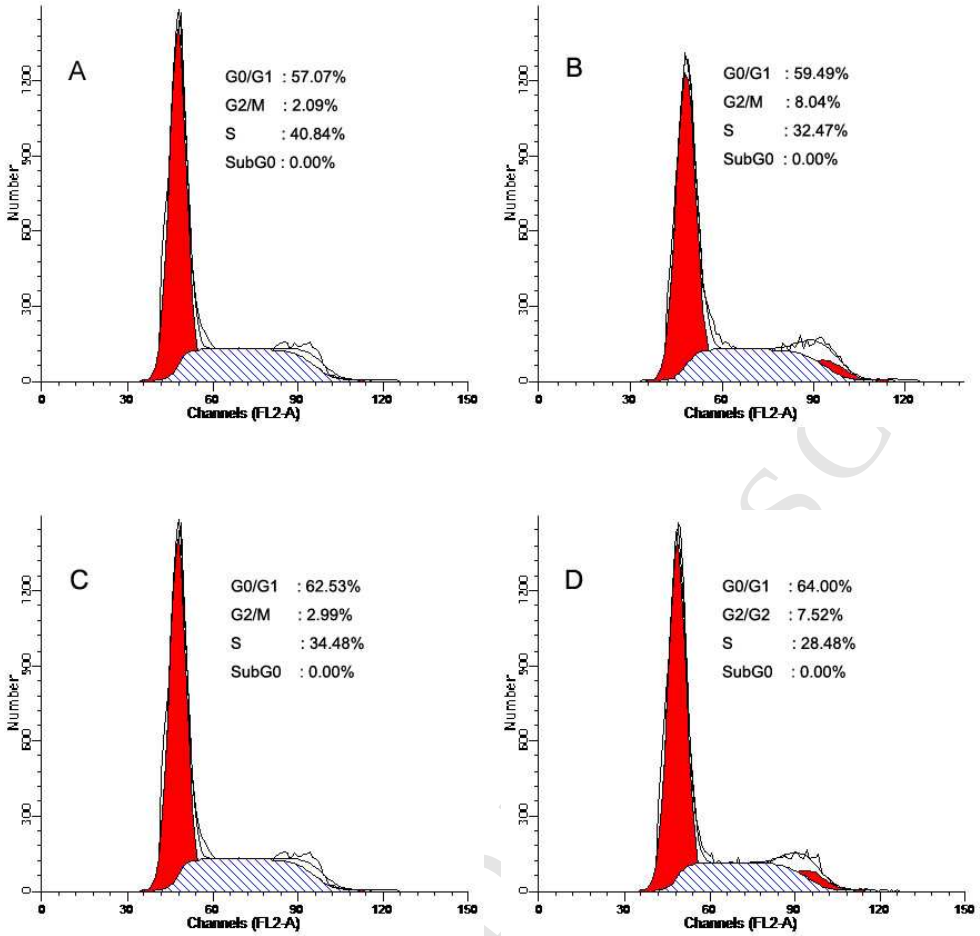

Figure 4. Effects of **10b** on the cell cycle distribution in A549 cells. A549 cells were treated with various concentrations of **10b**. A) control; B) concentrations of **10b** was 0.5 μM; C) concentrations of **10b** was 1.0 μM; D) concentrations of **10b** was 2.0 μM. A549 cells were treated with alcohol for 36 h as a control group, Values represent the mean ± S.D, n =3. P <0.05 versus control.

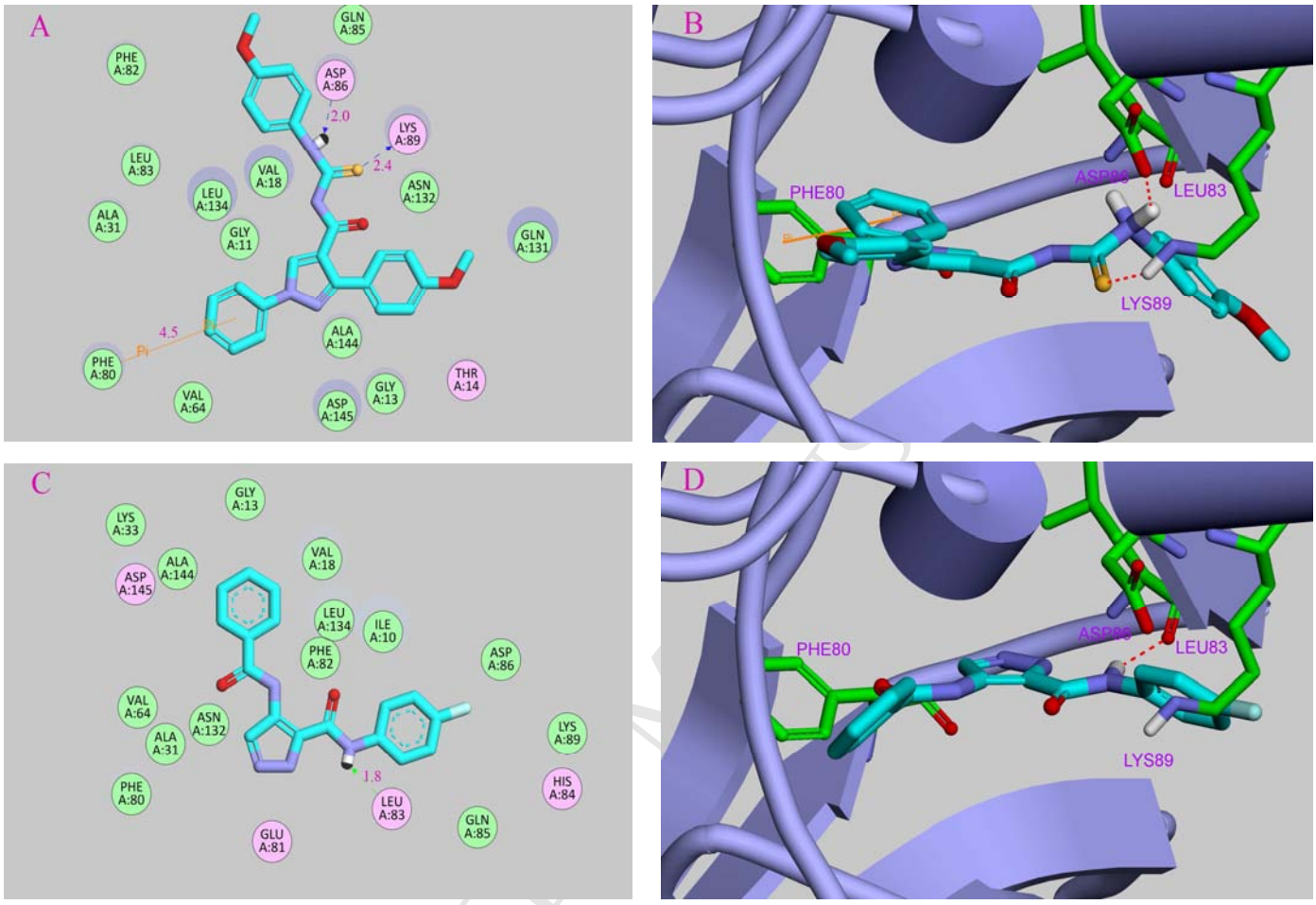

Figure 5. A) 2D molecular docking model of compound **10b** with 2VTO; B) Model of compound **10b** bound to CDK2; C) The 2D diagram of docking structure of LZ8 with 2VTO; D) Model of compound **LZ8** bound to CDK2.

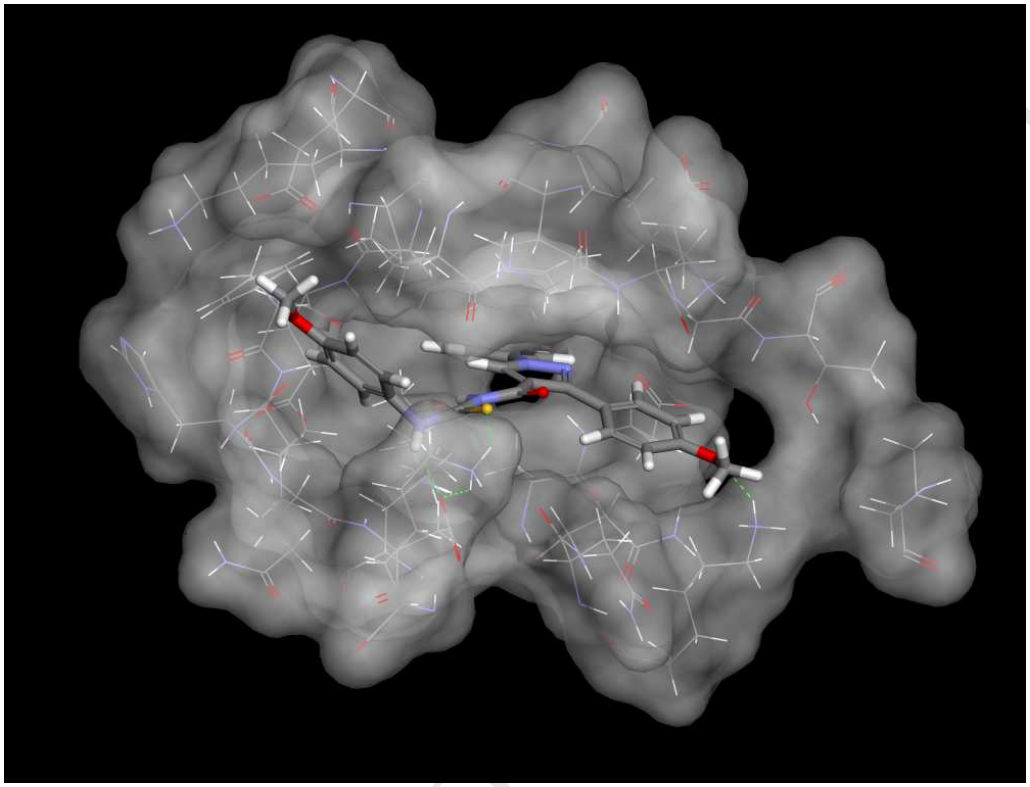

Figure 6. The surface model of compound **10b** with 2VTO

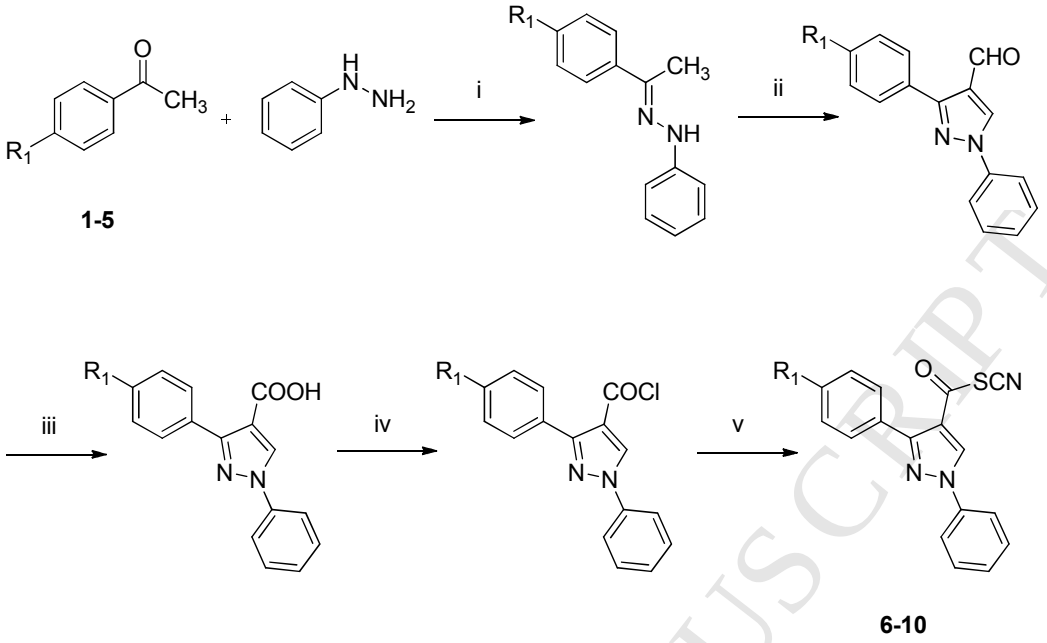

Scheme 1. Synthesis of compound **6-10**

Reagents and conditions: (i) ethanol, 50-60 °C, 3h; (ii) DMF, $POCl_3$, 50-60 °C, 5 h; (iii) $KMnO_4$, 70-80 °C, 3 h; (iv) $SOCl_2$, toluene, 70-80 °C, 3h; (v) NH_4SCN, 3% TBAB, acetone, rt, 1 h.

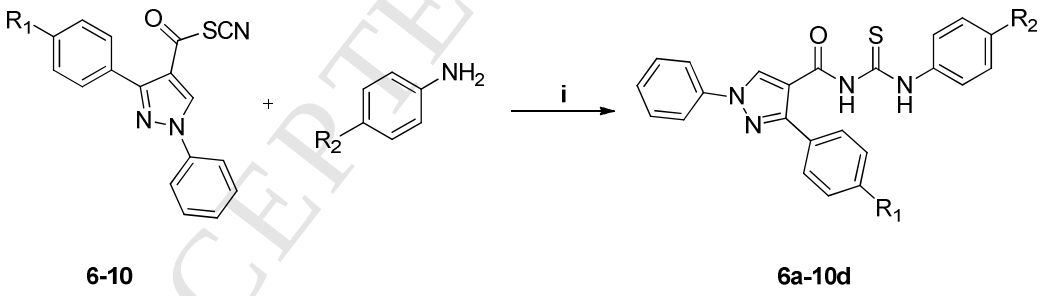

Scheme 2. Synthesis of compounds **6a-10d**

Reagents and conditions: (i) CH_2Cl_2, K_2CO_3, rt,1 h.

> Twenty novel pyrazole derivatives had been synthesized.

> The compounds were evaluated for brand-range CDKs inhibitory activity.

> Crystal structure of compound **7a** was determined.

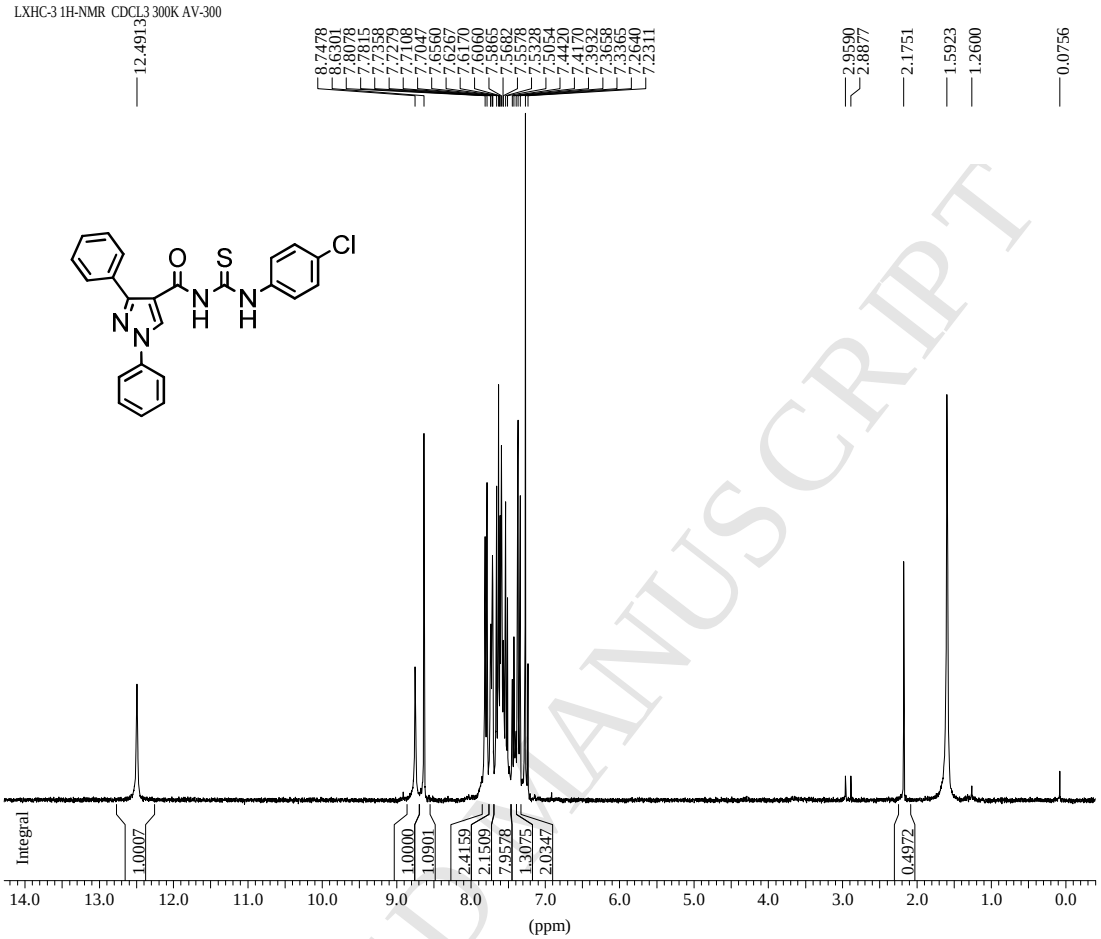

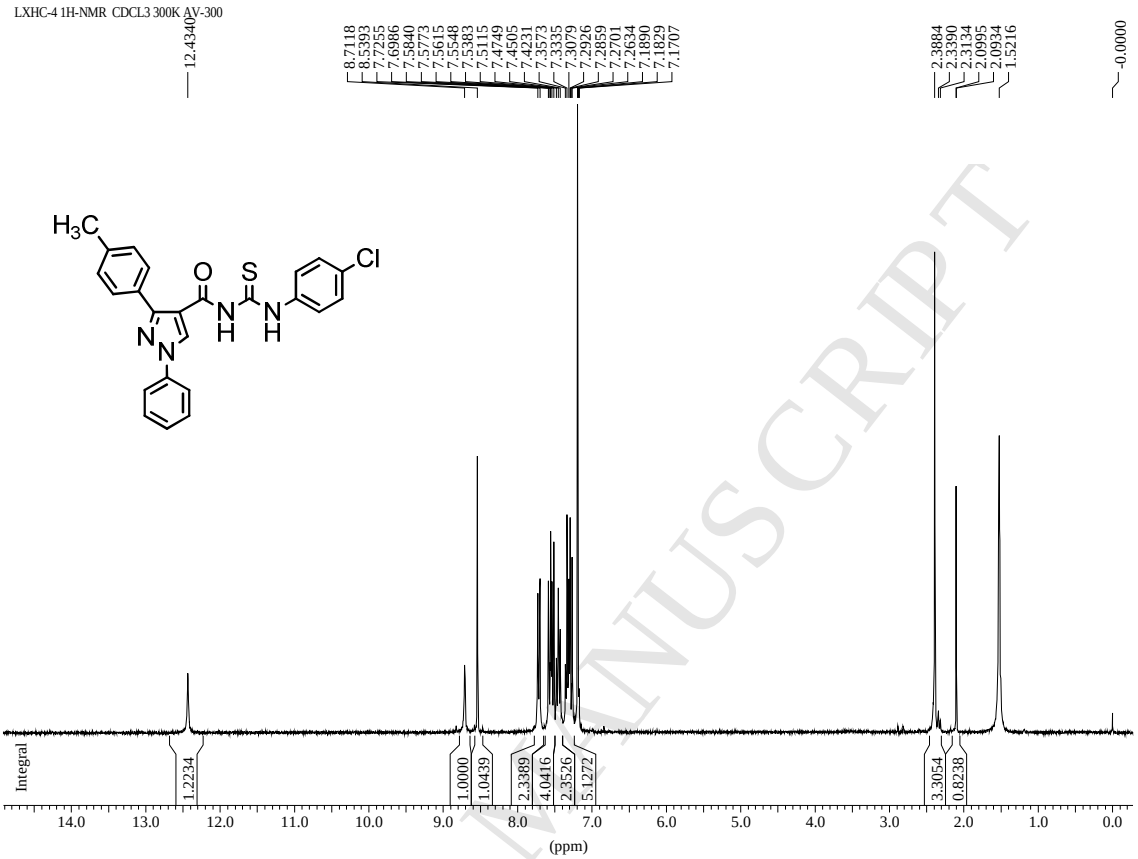

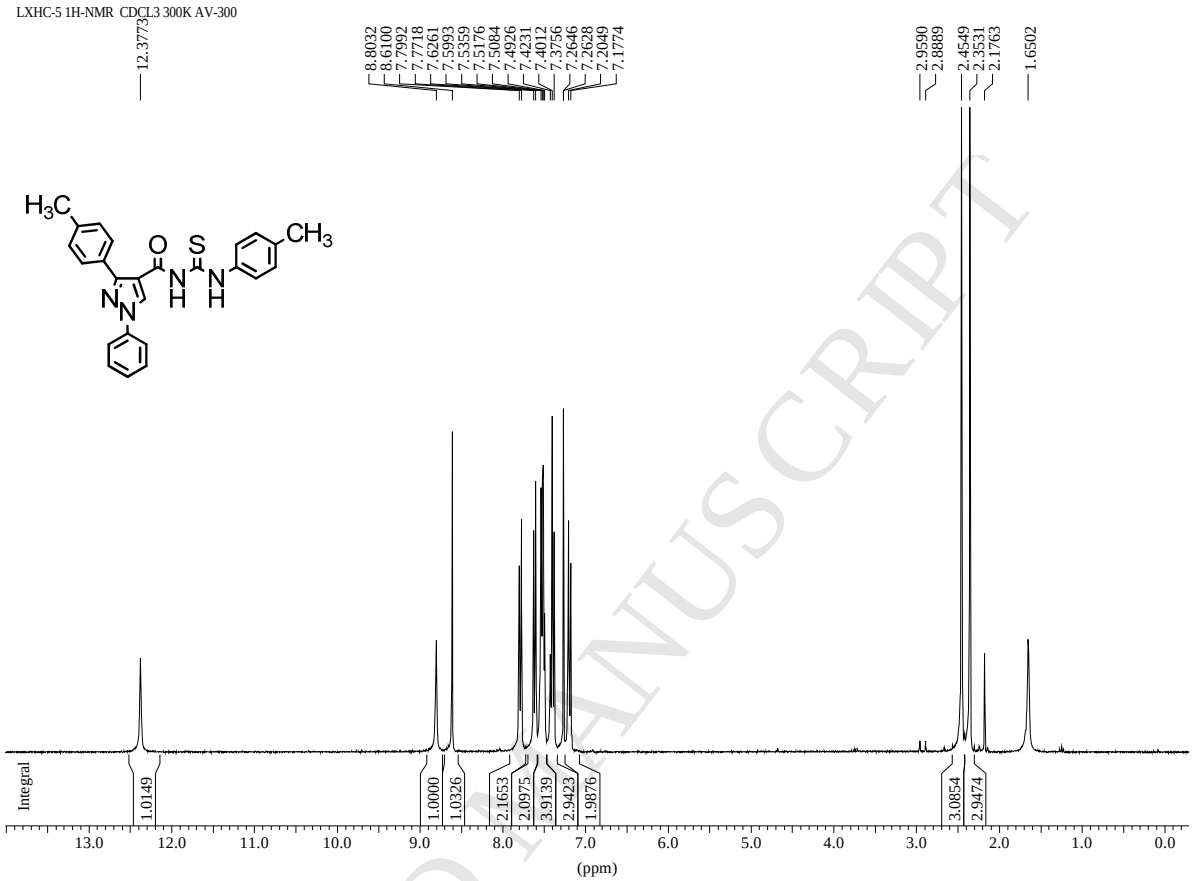

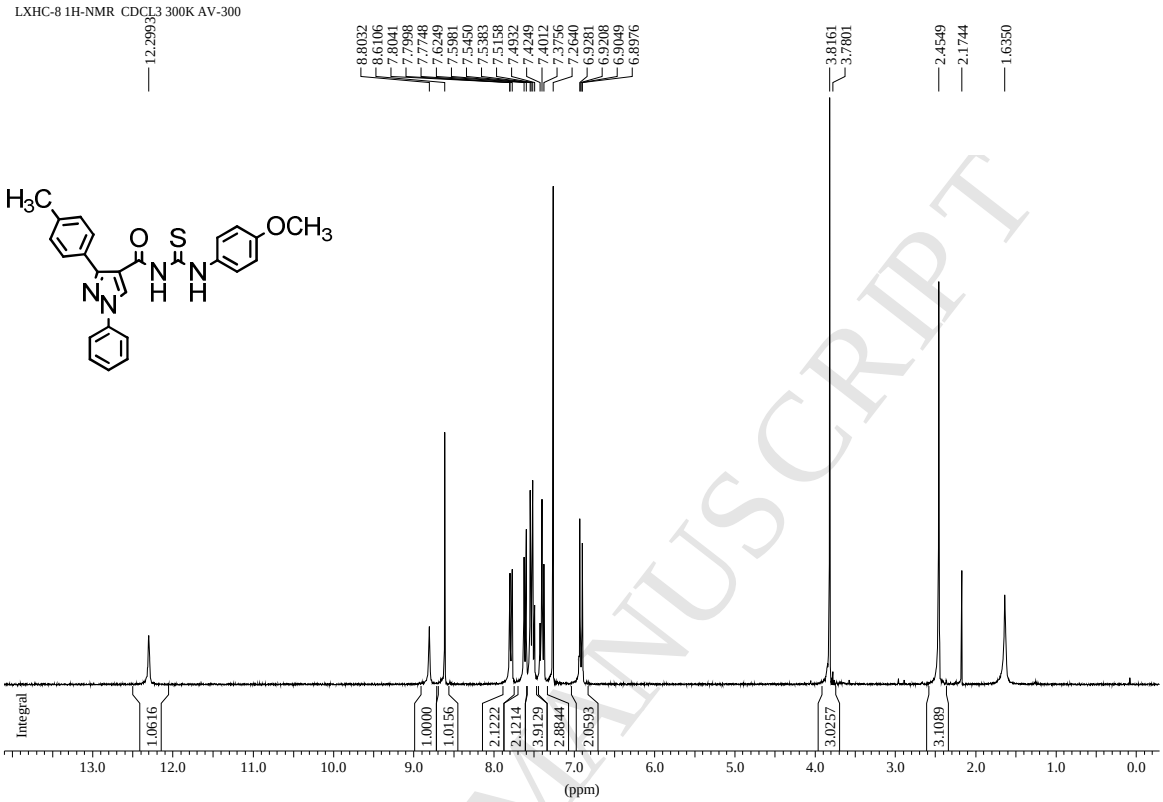

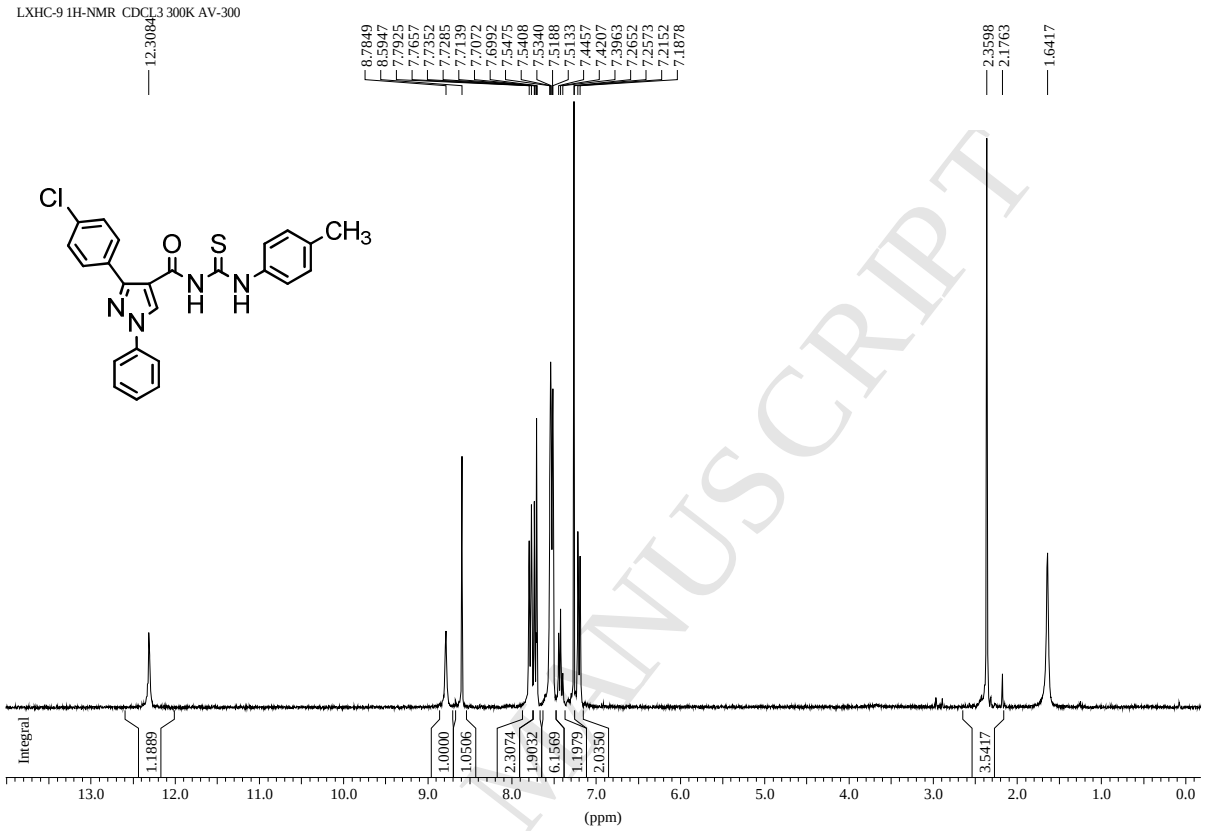

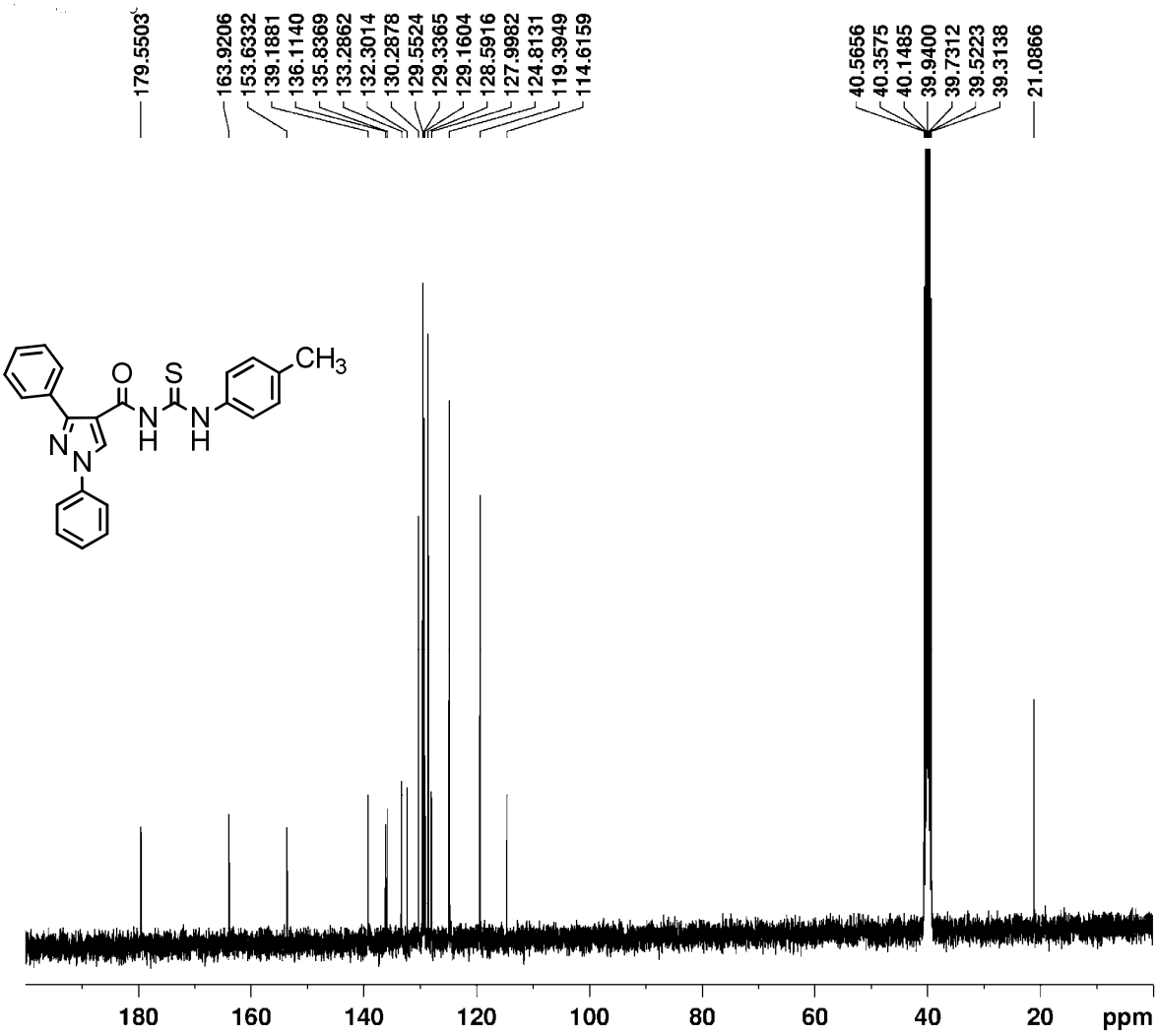
179.5503
163.9206
153.6332
139.1881
136.1140
135.8369
133.2862
132.3014
130.2878
129.5524
129.3365
129.1604
128.5916
127.9982
124.8131
119.3949
114.6159
40.5656
40.3575
40.1485
39.9400
39.7312
39.5223
39.3138
21.0866
O
S
N
H
N
H
N
N
CH3
180
160
140
120
100
80
60
40
20
ppm

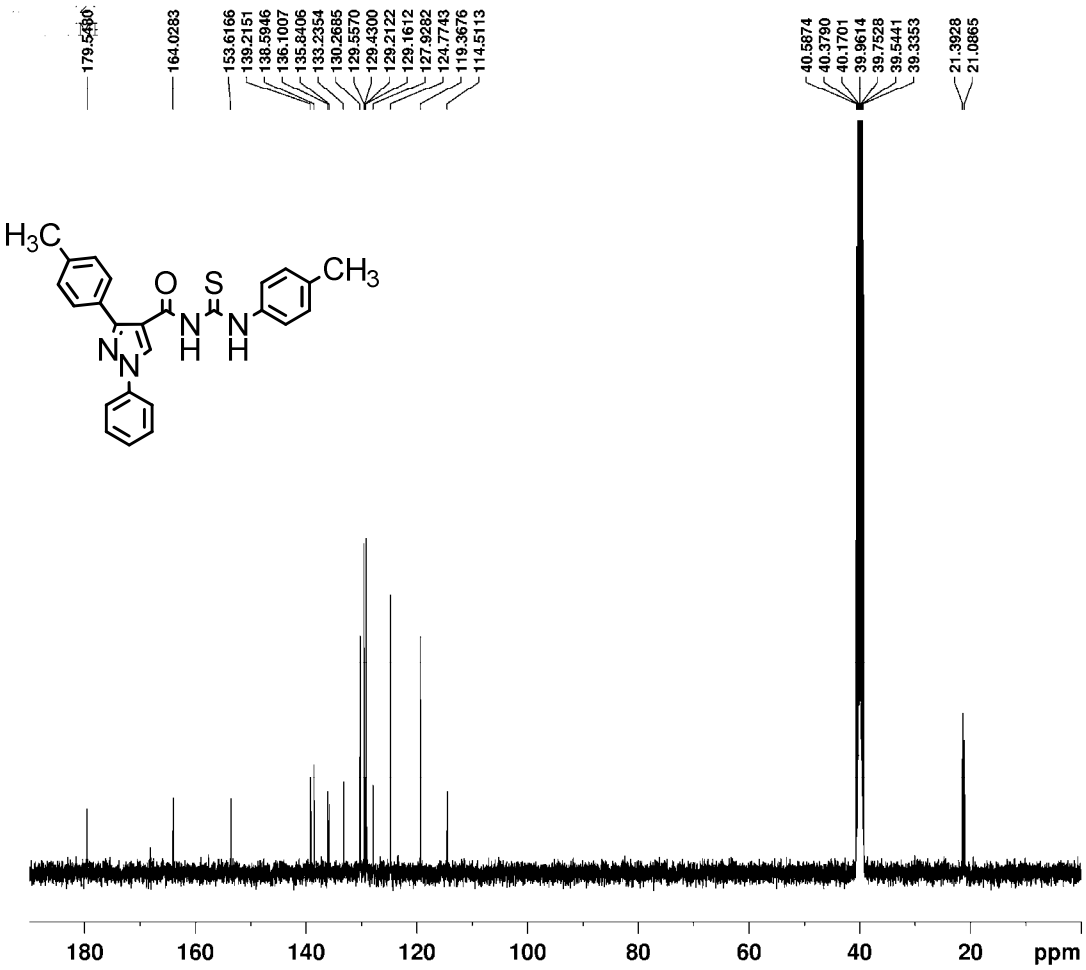
179.5490
164.0283
153.6166
139.2151
138.5946
136.1007
135.8406
133.2354
130.2685
129.5570
129.4300
129.2122
129.1612
127.9282
124.7743
119.3676
114.5113
40.5874
40.3790
40.1701
39.9614
39.7528
39.5441
39.3353
21.3928
21.0865
H3C
CH3
O
S
N
H
N
H
N
180
160
140
120
100
80
60
40
20
ppm